2024 European Control Conference (ECC)
June 25-28, 2024. Stockholm, Sweden

A Predictive Operation Management Scheme for Hydrogen Networks Based on the Method of Characteristics

Ulrike Herrmann[1], Anton Plietzsch[1], Max Rose[1], Hannes Gernandt[1], Johannes Schiffer[1,2]

***Abstract*— As future hydrogen networks will be strongly linked to the electricity system via electrolysers and hydrogen power plants, challenges will arise for their operation. A suitable response to phenomena, such as rapidly changing boundary conditions and unbalanced supply and demand, requires the implementation of operational concepts based on transient pipe models. The transient pipe flow can be described by the isothermal Euler equations, which we discretize using an explicit Method Of Characteristics. Based on this, we develop a nonlinear space-time discretized network model that incorporates various other components, including hydrogen storage facilities, active elements such as valves and compressor stations, as well as electrolyzers and fuel cells. This network model serves as the foundation for the development of a tailored economic model predictive control algorithm designed for fast timescales. The algorithm enables controlled pressure changes within specified bounds in response to changes in supply and demand while simultaneously minimizing fast pressure fluctuations in the pipelines. Through a detailed case study, we demonstrate the algorithm's proficiency in addressing these transient operation challenges.**

I. INTRODUCTION

Plans for the development of dedicated hydrogen networks in Europe are progressing steadily [1]. These future hydrogen networks will be coupled to the electric power grid through electrolyzers and hydrogen power plants. This coupling might introduce operational challenges, such as rapid fluctuations in hydrogen production and consumption and unbalanced supply and demand, primarily stemming from the inherent variability of renewable energy sources. However, unlike electricity grids, gas networks have the capability to store energy within specific line sections for limited durations by adjusting pipe pressure within operational limits, a process known as 'line pack storage' [2]. Transient models are needed to capture those line pack effects as well as the dynamic transients caused by rapid fluctuations of supply or demand. The transient modeling of pipeline flow is associated with the challenge of solving a set of nonlinear partial differential equations, the so-called Euler equations. Work on this topic has so far only been carried out in the field of natural gas networks, see [2], [3], [4], [5], [6], [7]. The aim of this paper is to open up the field for the transient modeling and optimization of hydrogen networks.
A detailed model catalog outlining different assumptions for the Euler equations in the context of gas networks can be found in [8]. As one-dimensional pipe flow and isothermal conditions are assumed in all the above-mentioned publications on transient gas network modeling, we refer in the following only to the one-dimensional, isothermal Euler equations. Beyond that, the distinction between slow and fast boundary transients is important for the assumptions that can be made regarding the Euler equations [2] as well as for a suitable choice of the discretization method [9]. Slow boundary transients are associated with changes in the boundary conditions, i.e. supply and demand, in the timescale of hours or on a daily cycle [9], [10] and thus with "normal" natural gas network operation [2]. Fast boundary transients are associated with rapid changes in the boundary mass flow or pressure, e.g. from the start-up or shut-down of a plant or the failure of a compressor [9], [10]. In contrast to the above-mentioned work on natural gas, which mostly considers slow transients, we will focus our work on fast transients for two reasons. First, in hydrogen networks frequent start-ups and shut-downs of electrolyzers and hydrogen power plants are to be expected, as these technologies base their operation on the supply or undersupply of renewable energy, repectively. Second, hydrogen presence in steel pipes can lead to material-related problems, the severity of which depends on the frequency and intensity of pressure fluctuations [11].
To solve the Euler equations numerically, a spatio-temporal discretization is necessary. The most common methods for spatial discretization are the Finite Differences Method (FDM), Method Of Characteristics (MOC), and Finite Volume Method (FVM). An FDM approach for gas network optimization is used in [12] and in [4]. In a recent study, the authors in [13] utilize an FDM-based lumped parameter approach, inspired by the Π-model used for transmission lines in the power network domain. They succeed in establishing a port-Hamiltonian system for the transient modeling of natural gas networks. However, their work primarily focuses on slow transients. Burlacu et al. [3] use FVM discretization which in general is well suited for both slow and fast transients [14]. Yet, they make assumptions regarding the isothermal Euler equations that are oriented at slow transients as well. A MOC approach suitable for modelling fast transients is suggested in [15]. MOC is associated with good accuracy and in some cases improved stability compared to FDM [15] as well as the proper setting of boundary conditions [9].
On the basis of the MOC model, we develop a control algorithm that adapts the operation of the hydrogen network to frequently changing supply and demand, while at the same time minimizing the pressure fluctuations in the pipeline to prevent premature material fatigue. To achieve this goal, we develop an economic model predictive control (EMPC)

[1]Fraunhofer IEG, Fraunhofer Research Institution for Energy Infrastructures and Geothermal Systems IEG, 03046 Cottbus, Germany, ulrike.herrmann@ieg.fraunhofer.de
[2]Brandenburg University of Technology Cottbus-Senftenberg, 03046 Cottbus, Germany, schiffer@b-tu.de

Copyright ©2024 EUCA

scheme, see e.g. [16]. Unlike setpoint tracking model predictive control (MPC), EMPC allows specific performance targets to be achieved under changing boundary conditions without necessarily reaching one or more steady states. This method is well-suited for the task, enabling explicit minimization of temporal pressure change rates in pipes while ensuring pressure remains within operational limits. Additionally, the predictive approach allows the incorporation of knowledge on the system's disturbances, i.e. predicted time series data related to hydrogen production and consumption. The contributions of this work are the following: First, building on the work of [15], we develop a high-resolution spatial and temporal discretization of the nonlinear 1D Euler equations for hydrogen pipelines. Additional simplifying assumptions applied to the Euler equations, along with the discretization method using MOC, are tailored to analyze fast transients effectively. Secondly, we enable a sector-coupled analysis by providing a network description combining the transient pipe model with simple models for hydrogen storage, electrolyzers, fuel cells, and active elements such as compressor stations and valves. The network model is given as a time-discrete non-linear state space model with spatially distributed states. Third, we present an EMPC approach for the control of the active elements on fast timescales, which allows for some line pack flexibility while keeping pipe pressures within certain operational bounds and minimizing the temporal pressure change rates in the pipe. The effectiveness of our approach is then demonstrated in a case study.

The paper is organized as follows: In Section II, we introduce models for all components of a hydrogen network. In Section III a discretized model for hydrogen networks is derived using the Method Of Characteristics. In Section IV we explore the development of an EMPC system for managing fast network dynamics. The control algorithm is examined through a small case study in Section V. Lastly, in Section VI we critically examine the results and provide insights into potential future research directions.

NOTATION

Let $\mathbb{R}$, $\mathbb{R}^+$ and $\mathbb{N}$ denote the real, non-negative real and natural numbers, respectively. For a finite set $\mathcal{S}$, $|\mathcal{S}|$ denotes its cardinality.

II. HYDROGEN NETWORK MODELING

In this section, we derive a model describing the flow dynamics of hydrogen networks that serves as a basis for the EMPC scheme. To this end, we consider hydrogen networks consisting of pipes that transport hydrogen between junctions, pressurized storage and flow control elements, i.e. control valves and compressor stations. Additionally, external fuel cells can extract and external electrolyzers can inject hydrogen from the junctions and storage facilities. We represent the topology of the hydrogen network by a connected and directed graph $\mathcal{G} = (\mathcal{N}, \mathcal{E})$, where $\mathcal{N} = \{v_1, \dots, v_{|\mathcal{N}|}\}$ denotes the set of nodes and $\mathcal{E} = \{e_1, \dots, e_{|\mathcal{E}|}\}$ denotes the set of edges. An edge $e = (v, w) \in \mathcal{E}$ exists, if it points from $v \in \mathcal{N}$ to $w \in \mathcal{N}$ for $v \neq w$. Each edge is either associated with a pipe $p \in \mathcal{E}_\mathrm{p} \subset \mathcal{E}$ or a flow control element $c \in \mathcal{E}_\mathrm{c} \subset \mathcal{E}$, i.e., a control valve or compressor station, such that $\mathcal{E} = \mathcal{E}_\mathrm{p} \cup \mathcal{E}_\mathrm{c}$. Each node is either associated with a storage $s \in \mathcal{N}_\mathrm{s} \subset \mathcal{N}$ or a junction $u \in \mathcal{N}_\mathrm{u} \subset \mathcal{N}$, such that $\mathcal{N} = \mathcal{N}_\mathrm{s} \cup \mathcal{N}_\mathrm{u}$.

Transient pipe model

In order to formulate the isothermal Euler equations, which describe the dynamics of gas flow within pipes [15], we assign a one-dimensional spatial variable, pressure, and mass flow to each pipe. Additionally, the hydrogen within the pipe is characterized by its density. Consequently, an edge $e \in \mathcal{E}$ is associated with a spatial variable $x^e \in [0, L^e] \subseteq \mathbb{R}^+$, where $L^e > 0$ denotes the length of the edge, a pressure $p^e(x^e, t) \in \mathbb{R}^+$, a mass flow $q^e(x^e, t) \in \mathbb{R}$, and a density $\rho^e(x^e, t) \in \mathbb{R}^+$. For simplicity, we omit explicit mentioning of the spatial variable and time dependence in the subsequent discussion, whenever it is evident from the context. The relationship between mass flow and density for a pipe $e \in \mathcal{E}_\mathrm{p}$ is defined through the hydrogen flow velocity $v^e(x^e, t) \in \mathbb{R}$, such that $q^e = A^e \rho^e v^e$, where the cross-sectional area of the pipe $A^e \in \mathbb{R}^+$ is assumed to be constant. Furthermore, pressure and density are connected through the isothermal equation of state for real gases:

$$p^e = \rho^e R_\mathrm{s} T z(p, T), \tag{1}$$

where $T \in \mathbb{R}^+$ is the constant gas temperature, $R_\mathrm{s} \in \mathbb{R}^+$ is the specific gas constant and $z(p, T) \in \mathbb{R}^+$ is the compressibility factor. For the transient modeling of hydrogen pipelines, we follow a number of assumptions that are frequently made in the literature on natural gas pipelines and comment below on their validity for hydrogen.

Assumption 2.1: (i) The isothermal compressibility factor is independent from the pressure, i.e., $z(p, T) = z(T) = const.$. (ii) The convective acceleration of hydrogen is negligible. (iii) Gravitational forces are negligible. (iv) The flow regime is fully rough, which means that the Darcy-Weisbach friction factor $\lambda \in \mathbb{R}^+$ depends only on the relative roughness of the pipeline [8]. (v) The isothermal speed of sound within hydrogen $c_s \in \mathbb{R}^+$ is constant.

The error of assuming a constant compressibility factor (Assumption 2.1 (i)) is small for hydrogen pressures up to $p \leq 100\,\mathrm{bar}$ [17], [18]. It should be noted that the compressibility factor of hydrogen - in contrast to most other gases including natural gas - is greater than one for temperatures relevant for pipeline operation [18]. Assumption 2.1 (ii) is usually made for natural gas pipelines because the flow velocity is significantly smaller than the speed of sound c_s [3], [2]. This assumption also holds for hydrogen pipes as the speed of sound in hydrogen is roughly three times higher than the speed of sound in natural gas [19]. The neglect of gravitational forces (Assumption 2.1 (iii)) is often made in the literature on gas network optimization [3], [2], [4] and is applicable to pipelines with no or a small angle of inclination [8]. Assumption 2.1 (iv) is made for example in Burlacu et al. [3] and is accurate for high Reynolds numbers for both natural gas and hydrogen flows [8]. The isothermal speed

of sound is defined as $c_s = \sqrt{p/\rho} = \sqrt{R_s T z}$. A constant isothermal speed of sound (Assumption 2.1 (v)) follows from Assumption 2.1 (i) for both natural gas [3], [8] and hydrogen [20] pipelines. An additional common assumption in natural gas networks is the consideration that the time variation of mass flow is significantly smaller than the friction effects, giving rise to the friction-dominated model [2], [8], [3]. However, this assumption is not applied here, due to its unsuitability for rapid boundary transients [2].

Using Assumption 2.1, the conservation of mass and the conservation of momentum of a pipe $e \in \mathcal{E}_\mathrm{p}$ read

$$\begin{aligned} 0 =& \partial_t p^e + \frac{c_s^2}{A^e}\partial_x q^e, \\ 0 =& \partial_t q^e + A^e \partial_x p^e + \frac{\lambda^e}{2A^e D^e}\left(\rho^e\right)^{-1} q^e |q^e|, \end{aligned} \tag{2}$$

where $D^e \in \mathbb{R}^+$ denotes the diameter of the pipeline [8].

Flow control elements

Flow control elements represent devices, such as control valves or compressor stations, which are represented by an edge $e \in \mathcal{E}_\mathrm{c}$ and preserve the in- and outgoing mass flow, i.e.,

$$q^e(t) = q^e(0,t) = q^e(L^e,t), \quad t \geq 0. \tag{3}$$

We assume the dynamics of the flow control elements to be fast compared to the flow dynamics in the pipes. Thus, we model flow control elements in steady state and allow for directly controlling the mass flow in (3).

Storage and junction model

Nodes $v \in \mathcal{N}$ describing storage facilities or junctions are assigned with a volume $V^v \in \mathbb{R}^+$ and a node pressure $p^v(t) \in \mathbb{R}^+$, which is assumed to be spatially uniformly distributed. For a node $v \in \mathcal{N}$, we collect all incoming and outgoing edges in the sets $\delta_v^+ = \{e \in \mathcal{E} : e = (v,w)\}$ and $\delta_v^- = \{e \in \mathcal{E} : e = (w,v)\}$, respectively. Then, we can write the conservation of mass at node $v \in \mathcal{N}$ in the following way

$$\frac{V^v}{R_\mathrm{s} T z}\frac{dp^v(t)}{dt} = \sum_{k \in \delta_v^+} q^k(0,t) - \sum_{l \in \delta_v^-} q^l(L^l,t) + q^v(t), \tag{4}$$

where $q^v(t) \in \mathbb{R}$ denotes a mass flow that is externally injected into or extracted from node $v \in \mathcal{N}$. Here we consider mass flows injected by an electrolyzer $q^{\mathrm{ely},v}$ as well as mass flows extracted by a fuel cell $q^{\mathrm{fc},v}$ or a hydrogen demand $q^{\mathrm{dem},v}$

$$q^v(t) = q^{\mathrm{ely},v}(t) + q^{\mathrm{fc},v}(t) + q^{\mathrm{dem},v}(t). \tag{5}$$

In the following, storage and junction nodes are distinguished by their volume. The volume of a junction $u \in \mathcal{N}_\mathrm{u}$ is rather small compared to a storage $s \in \mathcal{N}_\mathrm{s}$. For the modelling we therefore assume that $V^u \approx 0$ holds. With this assumption, the general mass balance in (4) can be written for junctions as the algebraic coupling condition used e.g. in [3] and [8]. Furthermore, for all nodes $v \in \mathcal{N}$ the following coupling condition between the node pressures and the inlet and outlet pressures of the edges is used

$$p^i(t,0) = p^v(t),\ i \in \delta_v^+, \quad p^k(t,L^e) = p^k(t),\ k \in \delta_v^-. \tag{6}$$

Sector coupling components

Through the external mass flows in (5), associated to the electrolyzers and fuel cells, we achieve a coupling between the hydrogen and the electricity network, which might transfer power fluctuations from the electricity grid to the hydrogen network or vice versa. To describe the sector coupling, we consider at some nodes $v \in \mathcal{N}$ a simple algebraic relationship between the exchanged hydrogen mass flows and the corresponding electric powers $P^{\mathrm{ely},v} \in \mathbb{R}^+$ and $P^{\mathrm{fc},v} \in \mathbb{R}^-$ of the electrolyzers and fuel cells, respectively, i.e.

$$q^{\mathrm{ely},v} = \frac{\eta^{\mathrm{ely}} P^{\mathrm{ely},v}}{H_{H_2}}, \quad q^{\mathrm{fc},v} = \frac{P^{\mathrm{fc},v}}{\eta^{\mathrm{fc}} H_{H_2}}, \tag{7}$$

where $\eta^{\mathrm{ely}}, \eta^{\mathrm{fc}} \in [0,1]$ are the lumped conversion efficiencies and $H_{H_2} \in \mathbb{R}^+$ is the lower heating value of hydrogen.

III. DISCRETIZED HYDROGEN NETWORK MODEL

For the EMPC scheme, a discretized model of the isothermal Euler equations is required. To this end, we first rewrite the Euler equations (2) for a pipeline $e \in \mathcal{E}_p$ in the following general form

$$\begin{aligned} &\partial_t \begin{pmatrix} p^e \\ q^e \end{pmatrix} + M^\mathrm{e} \partial_x \begin{pmatrix} p^e \\ q^e \end{pmatrix} + \begin{pmatrix} 0 \\ J^e(p^e,q^e) \end{pmatrix} = 0, \\ &M^\mathrm{e} = \begin{pmatrix} 0 & \frac{c_s^2}{A^e} \\ A^e & 0 \end{pmatrix}, \quad J^e(p^e,q^e) = \frac{\lambda^e R_\mathrm{s} T z}{2 p^e A^e D^e} q^e |q^e|. \end{aligned} \tag{8}$$

Note that the matrix M^e is indefinite with eigenvalues c_s and $-c_s$. Therefore the isothermal Euler equations are a hyperbolic system of partial differential equations (PDEs).

In order to numerically solve the Euler equations (8), we follow [15] and [10] and apply the meshed MOC, a discretization method that is suitable for describing fast transients. The MOC uses the eigenvalues and eigenvectors of the matrix M_e in (8) to obtain a system of ordinary differential equations (ODEs).

The obtained ODEs are valid along the characteristic lines, which are located in the space-time plane and are associated with the eigenvalues of M_e. The characteristic lines x_+^e and x_-^e associated with $\lambda_1 = c_s$ and $\lambda_2 = -c_s$ are called forward and backward characteristics, respectively, and they are described by [15]

$$x_+^e(t) = c_s t + x_0^e, \quad x_-^e(t) = -c_s t + x_0^e, \tag{9}$$

where $x_0^e \in [0, L^e]$ is the initial value. The solutions of (8) are then considered along both characteristic lines, which leads to the following system of ODEs [15]

$$\begin{aligned} &\frac{A^e}{c_s}\frac{dp^e}{dt}(t, x_+^e(t)) + \frac{dq^e}{dt}(t, x_+^e(t)) + J(p^e,q^e) = 0, \\ &\frac{-A^e}{c_s}\frac{dp^e}{dt}(t, x_-^e(t)) + \frac{dq^e}{dt}(t, x_-^e(t)) + J(p^e,q^e) = 0. \end{aligned} \tag{10}$$

Applying the forward Euler discretization to (10), we obtain

$$\begin{aligned}\frac{A^e}{c_s}\frac{p^e_{i,j}-p^e_{i-1,j-1}}{\Delta t}+\frac{q^e_{i,j}-q^e_{i-1,j-1}}{\Delta t}+J^e_{i-1,j-1}=0,\\ -\frac{A^e}{c_s}\frac{p^e_{i,j}-p^e_{i+1,j-1}}{\Delta t}+\frac{q^e_{i,j}-q^e_{i+1,j-1}}{\Delta t}+J^e_{i+1,j-1}=0,\end{aligned} \tag{11}$$

where $i \in \mathbb{N}$, $j \in \mathbb{N}$ are the spatial and temporal index, respectively, $\Delta t \in \mathbb{R}^+$ is the discrete time step-size and $J^e_{i,j} = J^e(p^e_{i,j}, q^e_{i,j})$ is the source term. Using the characteristics (9), we obtain a discrete spatial step-size $\Delta x \in \mathbb{R}^+$ with $\Delta x = c_s \Delta t$ and assume that Δt is chosen according to the pipe length L^e in such a way that $K_e := \frac{L^e}{\Delta x} \in \mathbb{N}$ holds.

By solving for $p^e_{i,j}$ and $q^e_{i,j}$ in (11), we obtain an explicit expression for $p^e_{i,j}$ and $q^e_{i,j}$, for all $j \geq 1$ and $0 < i < K_e$, i.e.,

$$\begin{aligned}p^e_{i,j} = &\frac{1}{2}\left(p^e_{i-1,j-1}+p^e_{i+1,j-1}\right)\\ &+\frac{c_s}{2A^e}\left(q^e_{i-1,j-1}-q^e_{i+1,j-1}\right)\\ &+\Delta t\frac{c_s}{2}(J^e_{i+1,j-1}-J^e_{i-1,j-1}),\end{aligned} \tag{12}$$

$$\begin{aligned}q^e_{i,j} = &\frac{1}{2}\left(q^e_{i-1,j-1}+q^e_{i+1,j-1}\right)+\frac{A^e}{2c_s}\left(p^e_{i-1,j-1}-p^e_{i+1,j-1}\right)\\ &-\Delta t\frac{A^e}{2}\left(J^e_{i-1,j-1}+J^e_{i+1,j-1}\right).\end{aligned} \tag{13}$$

To determine the mass flows and pressures from (12) and (13), it remains to further specify the initial values $p^e_{i,0}$ and $q^e_{i,0}$, for all $i = 0, \ldots, K_e$.

Furthermore, the boundary values $p^e_{0,j}$, $p^e_{K_e,j}$, $q^e_{0,j}$, and $q^e_{K_e,j}$ for all $j \geq 0$ are required. For the first time step, we assume that the initial node pressures p^v_0 at all nodes $v \in \mathcal{N}$ are given. Then, we determine the discretized node pressures at $v \in \mathcal{N}$ from an Euler discretization of (4) for all $j \geq 1$ via

$$\frac{p^v_j - p^v_{j-1}}{\Delta t}\frac{V^v}{R_s T z} = \sum_{e\in\delta^+_v} q^e_j - \sum_{e\in\delta^-_v} q^e_j + q^v_j, \tag{14}$$

where q^v_j denotes the incoming or outgoing mass flow from an electrolyzer, fuel cell, or hydrogen demand and the mass flows q^e_j exchanged via pipes or flow control elements are given by

$$q^e_j = \begin{cases} q^e_{K_e,j}, & \text{if } e \in \delta^+_v \cap \mathcal{E}_\mathrm{p},\\ q^e_{0,j}, & \text{if } e \in \delta^-_v \cap \mathcal{E}_\mathrm{p},\\ q^e_j, & \text{if } e \in \mathcal{E}_\mathrm{c}.\end{cases}$$

Based on (14), the pressures at the boundary points of the pipe are then given by

$$p^e_{0,j} = p^v_j,\ e \in \delta^-_v, \quad p^e_{K_e,j} = p^w_j,\ e \in \delta^+_w. \tag{15}$$

To calculate the node pressure p^v_j from (14), we replace the pipe mass flows $q^e_{K_e,j}$ and $q^e_{0,j}$ by using the forward and backward characteristic (11). Together with (15), this yields

$$\begin{aligned}q^e_{K_e,j} &= \frac{A^e}{c_s}\left(p^e_{K_e-1,j-1}-p^v_j\right)+q^e_{K_e-1,j-1}-\Delta t J^e_{K_e-1,j-1}\\ q^e_{0,j} &= \frac{A^e}{c_s}\left(p^v_j-p^e_{1,j-1}\right)+q^e_{1,j-1}-\Delta t J^e_{i+1,j-1}.\end{aligned} \tag{16}$$

This, together with (14), yields for each node $v \in \mathcal{N}$

$$\begin{aligned}p^v_j = \alpha\Bigg(&\frac{V^v}{R_s T z \Delta t}p^v_{j-1}+\sum_{e\in\delta^{\mathrm{p},+}_v}\tilde{q}^e_{K_e-1,j-1}-\sum_{e\in\delta^{\mathrm{p},-}_v}\tilde{q}^e_{1,j-1}\\ &+\sum_{e\in\delta^{\mathrm{c},+}_v}q^e_j-\sum_{e\in\delta^{\mathrm{c},-}_v}q^e_j-q^v_j\Bigg)\end{aligned} \tag{17}$$

with the sets of incoming and outgoing valves $\delta^{\mathrm{c},\pm}_v := \delta^\pm_v \cap \mathcal{E}_\mathrm{c}$ and the sets of incoming and outgoing pipes $\delta^{\mathrm{p},\pm}_v := \delta^\pm_v \cap \mathcal{E}_\mathrm{p}$. For readability reasons, we define the constant factor

$$\alpha = \left(\frac{V^v}{R_s T z \Delta t} + c_s^{-1}\sum_{e\in\delta^{\mathrm{p},+}_v\cup\delta^{\mathrm{p},-}_v} A^e\right)^{-1}$$

as well as for all $j \geq 0$ the artificial terms

$$\begin{aligned}\tilde{q}^e_{K_e-1,j-1} &= q^e_{K_e-1,j-1}+\frac{A^e}{c_s}p^e_{K_e-1,j-1}-A^e\Delta t J^e_{K_e-1,j-1}\\ \tilde{q}^e_{1,j-1} &= q^e_{1,j-1}-\frac{A^e}{c_s}p^e_{1,j-1}-A^e\Delta t J^e_{1,j-1}\end{aligned}$$

which can be interpreted as mass flows with regard to their physical unit and depend only on state variables from the previous time step $j-1$.

To summarize, we can model the flow dynamics within a hydrogen network using the equations (12), (13), and (17).

IV. ECONOMIC MODEL PREDICTIVE CONTROL

Based on the model outlined in Sections II and III, we develop an EMPC scheme to optimize hydrogen network operations by minimizing temporal pressure changes within the pipelines. This control approach guides the pipe flow towards steady state without imposing specific pressure or mass flow set points. To achieve this, we use the cost function

$$\ell(p^\mathrm{e}) = \sum_{e\in\mathcal{E}_\mathrm{p}}\sum_{i=1}^{K_e}\sum_{j=1}^{N}(p^e_{i,j}-p^e_{i,j-1})^2, \tag{18}$$

where $p^\mathrm{e} \in \mathbb{R}^d$, $d = \sum_{e\in\mathcal{E}_\mathrm{p}}(N+1)\cdot K_e$ denotes a vector collecting the pipeline pressures. Minimizing temporal pressure change rates is one of several objectives that can be addressed in the operation of hydrogen networks. We use it exemplary because it is specific to hydrogen networks and new compared to previous work on the operation of natural gas networks (see Section I). However, the described transient hydrogen network model can also be combined with the quadratic cost functions used in setpoint tracking MPC approaches [16].

To minimize (18) with respect to the discrete-time dynamics from Section III, we use the states of the system

$$(p^v_j)_{v\in\mathcal{N}},\ (p^e_{1,j}, q^e_{1,j}, \ldots, p^e_{K_e-1,j}, q^e_{K_e-1,j})_{e\in\mathcal{E}_\mathrm{p}}, \tag{19}$$

as optimization variables that are dynamically constraint by (12), (13) and (17) and the control inputs

$$(q^e_j)_{e\in\mathcal{E}_\mathrm{c}} \tag{20}$$

as independent optimization variables, see (3). The sector coupling components are not part of the optimization. Thus,

$$(P_j^{\mathrm{ely},v})_{v\in\mathcal{N}},\ (q_j^{\mathrm{fc},v})_{v\in\mathcal{N}},\ (q_j^{\mathrm{dem},v})_{v\in\mathcal{N}} \tag{21}$$

are disturbances to the system under consideration. In addition to the dynamic constraints, we impose the following box constraints for the optimization variables

$$p^v_{\min} \le p^v_j \le p^v_{\max}, \quad j \ge 0,\ v \in \mathcal{N} \tag{22}$$
$$p^e_{\min} \le p^e_{i,j} \le p^e_{\max}, \quad j \ge 0,\ i = 0,\dots,K_e,\ e \in \mathcal{E}_{\mathrm{p}} \tag{23}$$
$$q^e_{\min} \le q^e_{i,j} \le q^e_{\max}, \quad j \ge 0,\ i = 0,\dots,K_e,\ e \in \mathcal{E}_{\mathrm{p}} \tag{24}$$
$$q^e_{\min} \le q^e_j \le q^e_{\max}, \quad j \ge 0,\ e \in \mathcal{E}_{\mathrm{c}}. \tag{25}$$

Now, we can formulate the corresponding optimization problem that characterizes the EMPC scheme for hydrogen networks.

Problem 4.1 (Economic model predictive control scheme): At time $j = 0$, given initial states and control inputs (19) and (20) as well as known values for the disturbances (21) for $j = 1,\dots,N$, minimize (18) with respect to (19) and (20) such that (12), (13) and (17) as well as the box constraints (22)-(25) are satisfied.

Due to the nonlinearity of the source term $J^e_{i,j}$ in (12) and (13), the Problem 4.1 is a nonlinear optimization problem (NLP). The NLPs arising in MPC are commonly solved using IPOPT [16], which is also used to solve Problem 4.1 in our case study. From the obtained optimal sequence of the control variables in (20) only the first element is used. By repeating the optimization after each time step a closed-loop control law is then obtained.

V. Case Study

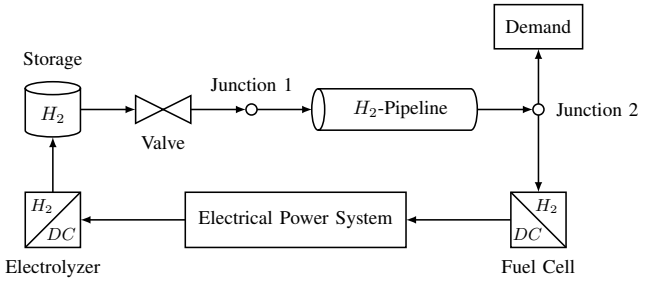

Fig. 1. Case study setup.

In this section, we present a simulation case study to demonstrate the effectiveness of the EMPC algorithm developed in the previous section. The case study focuses on a small hydrogen network, illustrated in Fig. 1, comprising three nodes (two junctions and one storage) and two edges (one valve and one pipeline). The simulation parameters are outlined in Table I. The closed-loop predictive operation management is implemented using Pyomo [21] and the IPOPT solver [22] for nonlinear optimization. The objective function (18) is designed to minimize temporal variation in the pipeline pressure, ensuring that the control steers the pipeline towards a steady state without imposing specific pressure setpoints. In order to represent the pressure fluctuations inside the pipeline, a spatial resolution was chosen such that the pipeline is discretized into five sections each of length $\Delta x = 5000\,\mathrm{m}$. Employing the MOC for discretizing the pipeline this spatial resolution leads to a temporal discretization of $\Delta t = \frac{\Delta x}{c_s} \approx 4.48\,\mathrm{s}$. The simulation scenario is intentionally kept simple to illustrate the model's behavior and the algorithm's capabilities. We assume perfect forecasts of disturbances, including mass flows from the electrolyzer, fuel cell, and demand. The simulation, depicted in Fig. 2, starts in a steady state, which can be obtained from the steady-state solution of (2), see [8]. In this initial state, the mass flow produced by the electrolyzer equals the demand and therefore mass is neither changing within the storage nor in the pipeline. After about $84\,\mathrm{s}$, a change in the disturbances occurs: the electrolyzer is deactivated, and the fuel cell is activated. Anticipating this change, the EMPC scheme adjusts the valve mass flow at the inlet of the pipeline. After the change, the demand at Junction 2 exceeds the maximum mass flow capacity of the valve between storage and pipeline. To balance this, hydrogen is not only withdrawn from the storage but also from the pipeline, consequently reducing its pressure. After about $250\,\mathrm{s}$ of the simulation time, the demand decreases, allowing the required mass flow at Junction 2 to be supplied entirely from the storage. This leads the pipeline to reach a steady state once more, though at a lower pressure than the initial state. This case study illustrates that the proposed algorithm is able to navigate through various operational conditions, effectively managing transient dynamics within the hydrogen network.

TABLE I

Overview of the parameter values used for the case study.

Parameter	Symbol	Value
Isothermal speed of sound	c_{s}	$1115.89\,m/s$
Specific gas constant	R_{s}	$4124\,J/(kgK)$
Compressibility factor	z	1.03
Lower heating value	H_{H_2}	$1.188 \cdot 10^8\,J/kg$
Temperature	T	$293.15\,K$
Prediction horizon	N	50
Temporal resolution	Δt	$4.48\,s$
Spatial resolution	Δx	$5000\,m$
Pipeline length	L	$2,5 \cdot 10^4\,m$
Pipeline diameter	D	$0.9\,m$
Pipeline roughness	r	$1 \cdot 10^{-4}\,m$
Storage volume	V	$20\,m^3$
Maximum valve flow	q_{max}	$5\,kg/s$

VI. Discussion and Outlook

In this paper, we have presented a discretized model for hydrogen networks using the Method Of Characteristics (MOC) for the discretization of gas transport dynamics. Utilizing this network model, we further developed an EMPC algorithm for managing fast boundary transients. The algorithm is based on a nonlinear optimization problem of minimizing the temporal change rates of pipeline pressures while keeping all the other state and control variables within their

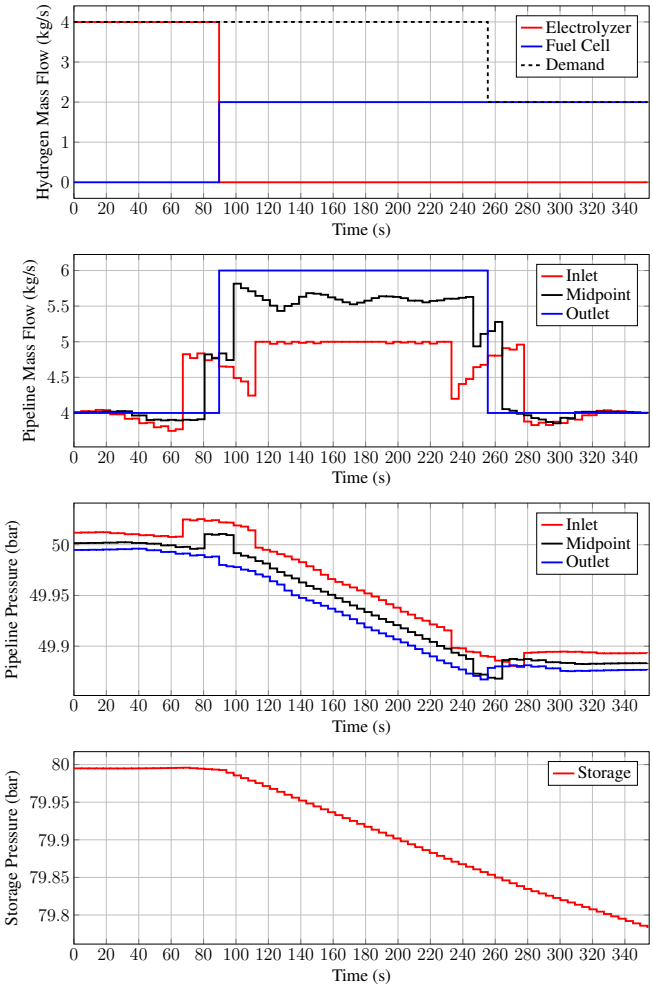

Fig. 2. Closed-loop EMPC case study of the network illustrated in Fig.1.

operational bounds. The EMPC scheme has been validated through a small simulation case study, demonstrating its ability to navigate through various operational conditions with rapid disturbances. However, there are several noteworthy aspects to consider regarding our methodology and potential areas for future improvement. Future research will focus on refining several assumptions made when modeling the hydrogen network. The constant friction coefficient, the neglect of gravitational forces, and the simplified representation of the electrolyzer and fuel cell are particularly noteworthy here. With the described network representation, our work enables the EMPC approach to be used for generic network topologies. In future work, we intend to further investigate the scalability of the central optimization approach for large networks. In addition, we seek to provide formal convergence and stability guarantees for the closed-loop system. In the EMPC context, stability is commonly demonstrated using dissipativity properties, see e.g. [16].

ACKNOWLEDGMENT

The authors gratefully acknowledge the financial support by the German Federal Ministry of Education and Research, as part of the public research projects TransHyDE (03HY201S) and EIZ (03SF0693E).

REFERENCES

[1] R. van Rossum, J. Jens, G. La Guardia, A. Wang, L. Kühnen, and M. Overgaag, "European hydrogen backbone: A european hydrogen infrastructure vision covering 28 countries," Guidehouse, Apr, 2022.
[2] L. A. Roald, K. Sundar, A. Zlotnik, S. Misra, and G. Andersson, "An uncertainty management framework for integrated gas-electric energy systems," Proceedings of the IEEE, vol. 108, no. 9, 2020.
[3] R. Burlacu, H. Egger, M. Groß, A. Martin, M. E. Pfetsch, L. Schewe, M. Sirvent, and M. Skutella, "Maximizing the storage capacity of gas networks: a global MINLP approach," Optimization and Engineering, vol. 20, no. 2, 2019.
[4] C. Liu, M. Shahidehpour, and J. Wang, "Coordinated scheduling of electricity and natural gas infrastructures with a transient model for natural gas flow," Chaos: An Interdisciplinary Journal of Nonlinear Science, vol. 21, no. 2, 2011.
[5] Y. Zhang, Z. Huang, F. Zheng, R. Zhou, X. An, and Y. Li, "Interval optimization based coordination scheduling of gas–electricity coupled system considering wind power uncertainty, dynamic process of natural gas flow and demand response management," Energy Reports, vol. 6, 2020.
[6] R. G. Carter and H. H. Rachford Jr, "Optimizing line-pack management to hedge against future load uncertainty," in PSIG annual meeting, 2003.
[7] S. Clegg and P. Mancarella, "Integrated modeling and assessment of the operational impact of power-to-gas (P2G) on electrical and gas transmission networks," IEEE Transactions on Sustainable Energy, vol. 6, no. 4, 2015.
[8] P. Domschke, B. Hiller, J. Lang, V. Mehrmann, R. Morandin, and C. Tischendorf, "Gas network modeling: An overview," preprint, 2021.
[9] A. R. D. Thorley and C. H. Tiley, "Unsteady and transient flow of compressible fluids in pipelines—a review of theoretical and some experimental studies," Int. Journal of Heat and Fluid Flow, vol. 8, no. 1, 1987.
[10] B. Koo, "A novel implicit method of characteristics using pressure-referenced correction for transient flow in natural gas pipelines," Journal of Natural Gas Science and Engineering, vol. 104, 2022.
[11] M. Steiner, U. Marewski, and H. Silcher, "DVGW Project SyWeSt H2: Investigation of steel materials for gas pipelines and plants for assesment of their suitability with hydrogen," DVGW, Tech. Rep., 2023.
[12] S. Hossbach, M. Lemke, and J. Reiss, "Finite-difference-based simulation and adjoint optimization of gas networks," Mathematical Methods in the Applied Sciences, vol. 45, no. 7, 2022.
[13] A. J. Malan, L. Rausche, F. Strehle, and S. Hohmann, "Port-Hamiltonian modelling for analysis and control of gas networks," in 22nd IFAC World Congress, Yokohama, Japan, 2023.
[14] R. J. LeVeque, "Nonlinear conservation laws and finite volume methods," Computational Methods for Astrophysical Fluid Flow: Saas-Fee Advanced Course 27, 1998.
[15] P. J. Thomas, Simulation of Industrial Processes for Control Engineers. Elsevier, 1999.
[16] S. V. Rakovi and W. S. Levine, Handbook of Model Predictive Control, 1st ed. Birkhäuser Basel, 2018.
[17] D. Stolten and V. Scherer, Transition to renewable energy systems. John Wiley & Sons, 2013.
[18] S. Mihara, H. Sagara, Y. Arai, and S. Saito, "The compressibility factors of hydrogen-methane, hydrogen-ethane and hydrogen-propane gaseous mixtures," Short Communications, vol. 10, 1977.
[19] National Institute of Standards and Technology (NIST), U.S. Department of Commerce, "NIST Chemistry WebBook, SRD 69," 2023, accessed on 2023-11-06. [Online]. Available: https://webbook.nist.gov/
[20] X. Ma, X. Tang, Z. Wang, Q. Wang, and D. Gao, "Speed of sound in hydrogen isotopes derived from the experimental pvt data and an improved quantum law of corresponding state," Scientific Reports, vol. 10, 2020.
[21] W. E. Hart, J.-P. Watson, and D. L. Woodruff, "Pyomo: modeling and solving mathematical programs in Python," Mathematical Programming Computation, vol. 3, 2011.
[22] A. Wächter and L. T. Biegler, "On the implementation of an interior-point filter line-search algorithm for large-scale nonlinear programming," Mathematical programming, vol. 106, 2006.